

Epitaxial Layer Lifetime Characterization in the Frequency Domain

J. E. Park, D. K. Schroder, S. E. Tan, and B. D. Choi,
Department of Electrical Engineering
Center for Solid State Electronics Research
Arizona State University
Tempe, AZ 85287-5706

M. Fletcher, A. Buczkowski, and F. Kirscht
Mitsubishi America
1351 Tandem Ave
Salem, OR 97303

Abstract

Surface photovoltage (SPV) measurements are traditionally carried out under steady-state conditions to determine the minority carrier diffusion length. While this technique is very convenient for bulk wafer defect characterization, especially the detection of iron in boron-doped silicon wafers, it is poorly suited to characterize epitaxial layers that are typically much thinner than the diffusion length. We have developed the theory for frequency-dependent SPV measurements and have verified this theory with experimental data. We consider the various recombination/generation components in the semiconductor sample and determine the dependence on photon flux density, optical absorption coefficient, doping density, recombination and generation lifetime, and temperature. We show that optical excitation can be used for space-charge region recombination measurements, provided the optical generation rate is lower than the thermal generation rate thereby making such measurements useful for epitaxial layer characterization.

Introduction

It is difficult to characterize epitaxial layers through recombination lifetime or minority carrier diffusion length measurements because the layers are usually much thinner than the minority carrier diffusion length. We will discuss the various difficulties with the aid of Fig. 1. In Fig. 1(a) we show a p -type epitaxial layer on a p^+ substrate, with optical excitation as used for several conventional recombination lifetime measurements. Electron-hole pairs (ehp) are generated either in the epitaxial layer *and* the substrate with penetrating light or in the epi layer alone through short wavelength light. Excess carriers recombine in the epi layer itself, at the surface, at the epi-substrate interface, and in the substrate. The resultant lifetimes or diffusion lengths are effective values strongly influenced by recombination at the surface and at the epi/substrate interface. Even if the surface is oxidized to reduce surface recombination, the Si/SiO₂ interface can still be a strong contributor to the effective lifetime.

Let us consider the carriers to be reasonably well confined to the epi layer due to the minority carrier potential barrier at the epi/substrate interface. We take the epi layer lifetime as τ_{epi} , the surface lifetime as τ_{s1} and the epi/substrate interface lifetime as τ_{s2} . The effective lifetime is¹

$$\frac{1}{\tau_{eff}} = \frac{1}{\tau_{epi}} + \frac{1}{\tau_{s1}} + \frac{1}{\tau_{s2}} \approx \frac{1}{\tau_{epi}} + \frac{2s_{r1}}{t_{epi}} + \frac{2s_{r2}}{t_{epi}} \quad (1)$$

using $\tau_s \approx t_{epi}/2s_r$, where t_{epi} is the epitaxial layer thickness and s_r the surface or interface recombination velocity. The substrate lifetime is not included in Eq. (1), because the excess carriers are largely confined to the epi layer. Hence, it is included in the interface recombination velocity s_{r2} .

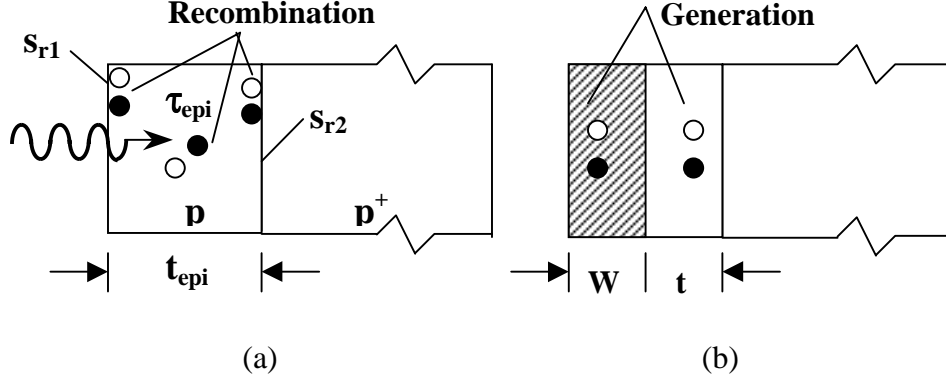


Fig. 1 Epitaxial layer lifetime characterization difficulties: (a) conventional recombination lifetime, (b) space-charge region lifetime measurements. t_{epi} : epi layer thickness, W : space-charge region width, t : quasi-neutral region width.

To illustrate the effect of surface/interface recombination on the recombination properties, we have plotted τ_{eff} versus epi layer thickness as a function of epi layer lifetime in Fig. 2, for $s_{r1} = s_{r2} = 1$ cm/s and 100 cm/s. For $t_{epi} < 4s_r t_{epi}$, the effective lifetime is dominated by interfacial recombination and for $t_{epi} > 4s_r t_{epi}$ by epitaxial layer recombination. For typical epi layer thicknesses of 10^{-4} to 10^{-3} cm, the effective lifetime is largely dominated by interfacial recombination for lifetimes of 10 μ s or higher for low s_r . The lifetime of high quality bulk Si wafers is typically in the 1-10 ms range. Epitaxial layers are likely to be slightly worse with lifetimes in the 100 μ s range due to slightly higher metallic contamination. Fig. 2 shows that in order to be able to say anything about the epi layer lifetime, even though the true lifetime may not be measurable, the surface recombination velocity has to be very low. Such low s_r can be achieved through effective chemical surface passivation or by driving the surface into accumulation with corona charge.²

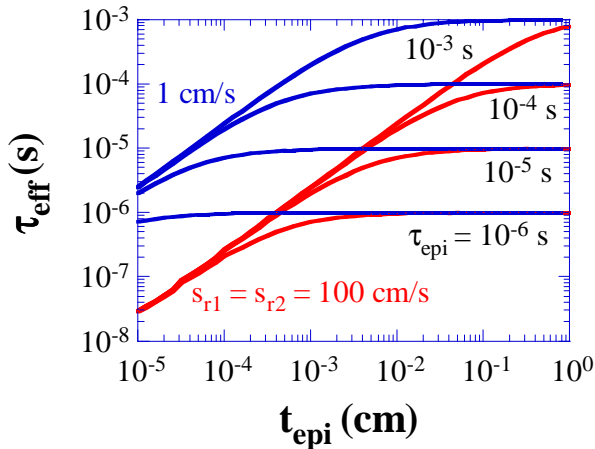


Fig. 2 Effective recombination lifetime versus epitaxial layer thickness as a function of epitaxial layer lifetime.

During surface photovoltage measurements, the ehps are generated in both regions, but the minority carrier diffusion length L_n in the heavily-doped substrate is usually much lower than that in the epi layer. Hence, the measurements typically yield t_{epi} rather than L_n . Due to these difficulties, space-charge region measurements are usually made with electron-hole pair generation/recombination largely confined to the scr. Such methods include measuring the leakage current of reverse-biased pn junctions,³ the recovery time of pulsed MOS capacitors,⁴ or the frequency dependence of a scr-dependent parameter.⁵ The emergence of commercially available charge-based semiconductor characterization tools has opened up the possibility of making such lifetime measurements on oxidized Si wafers without having to fabricate devices.⁶

Space-charge region based measurements can be augmented with optical excitation and contactless probe detection. Typically, a space-charge region is formed through an appropriate rinse of the sample or through surface charging. Low-intensity, high-absorption coefficient light ensures low-density electron-hole pair generation in the space charge region.⁷ The optically generated carriers lead to a slight forward bias, which in turn, leads to carrier injection into the quasi-neutral region. Hence, one needs to address scr and quasi-neutral region (qnr) recombination and generation. In addition, since carriers are generated near the surface, surface recombination also needs to be considered.

We present in this paper the relevant theory, supported by experimental data, of charge-based, light-excited contactless probe measurements of epitaxial layers. We show that for short wavelength light, with optically generated carriers largely confined to the space-charge region, we do, in fact characterize the epitaxial layer, through the *recombination lifetime* in the space-charge region.

Surface Charge/Probe

During charge-based measurements, charge is deposited on the wafer and the semiconductor response is measured by one of several techniques. Charge can be deposited from a corona source or through a chemical rinse. One can drive the corona-oxide-semiconductor (COS) device into deep depletion and measure the recovery transient with a contactless Kelvin probe.^{6,8} It is also possible to bias the COS device into inversion and measure the frequency response by varying the electrical signal applied to the Kelvin probe or by applying a time-varying optical signal to the device.⁵

To understand charge-based measurements, it is necessary to understand Kelvin probe measurements, first proposed by Kelvin probe in 1881.⁹ Kronik and Shapira give an excellent explanation of such probes and their various applications.¹⁰ A Kelvin probe is usually operated as a vibrating probe with minimization of the external current. The probes in some lifetime characterization instruments are not vibrating and we will refer to such probes as surface voltage probes. We will explain their operation with the aid of Fig. 3. Consider a p -type semiconductor with a grounded substrate. A metal probe, is placed a distance d (typically 0.1 – 1 mm) from the wafer surface. For simplicity, we assume the work functions of the probe and the semiconductor to be identical. With no surface charge on the semiconductor surface, the semiconductor bands are flat, as shown by the dashed energy band diagram in Fig. 3(a) and the probe potential, also known as the contact potential difference V_{cpd} , is zero.

For positive surface charge, the semiconductor is depleted, as shown by the solid energy band diagram in Fig. 3(a). The electrically floating probe will assume a positive contact potential difference V_{cpd} equal to the surface potential ϕ_s . With the semiconductor

illuminated, the Fermi level splits into two quasi-Fermi levels and both the semiconductor band bending and V_{cpd} are reduced, as illustrated in Fig. 3(b). Since we are dealing with optically-induced voltages in this paper, we will designate the probe voltage with illumination as the surface photovoltage V_{SPV} .

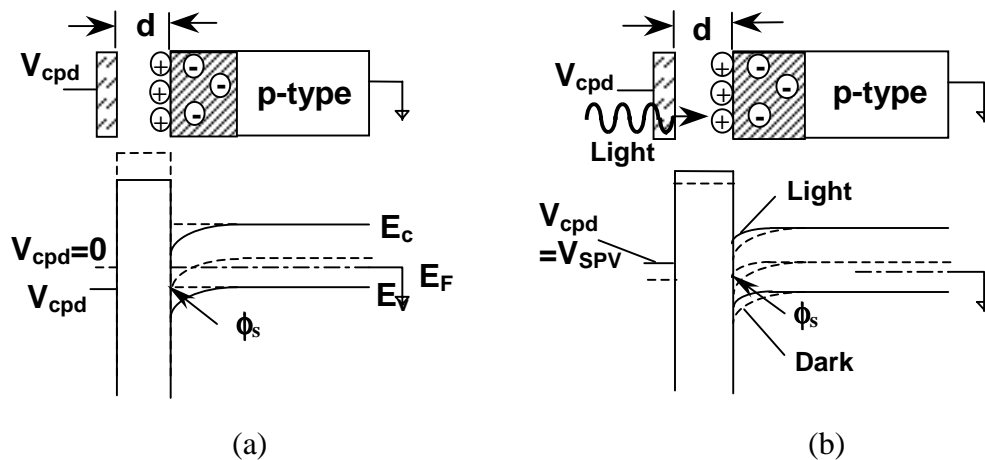


Fig. 3 Surface voltage probe energy band diagram: (a) in the dark and (b) with optical excitation.

A crucial component for SPV measurements is the surface treatment to create the surface space-charge region. Two options are available: deposit corona charge or treat the surface chemically. For *n*-type silicon, the oxide on the sample surface should be removed and then the sample should be boiled in H_2O_2 or in water for about 15 min and then rinsed in deionized water (DI).¹¹ Alternately, one can soak the sample in $KMnO_4$ for 1-2 min and then rinse in DI water. These treatments produce a stable depletion surface potential barrier. For *p*-type silicon very little treatment is required. In case of very low V_{SPV} , etching in buffered HF followed by a DI water rinse is recommended.

The energy band diagram of the probe-air-semiconductor system is analogous to that of a MOS capacitor with the insulator replaced with air. Positive charges, deposited on the semiconductor surface, deplete the surface of the *p*-type sample. Photons, incident on the sample, generate excess carriers within the space-charge region and in the quasi-neutral bulk region. The electrons within the scr and within a distance of approximately the minority carrier diffusion length from the edge of the scr will be collected in the space-charge region and reduce the surface potential barrier slightly. The barrier lowering is similar to a forward-biased junction and the probe detects the difference of the quasi-Fermi levels. For high-level injection, the surface potential vanishes and the probe achieves its maximum value.¹² However, we use low-level injection leading for low surface potentials.

Theory

We are considering the sample configuration of Fig. 4. Charge on the surface of the *p*-type wafer induces a space charge of width W . Incident light generates electron-hole pairs in the sample and the resulting surface photovoltage is measured. Where the carriers are generated depends on the wavelength of the incident light. We treat the general case of generation in both the space-charge region and in the quasi-neutral region. In general there is recombination of the excess carriers and generation of carriers. We consider both.

The equivalent circuit concept is very effective in understanding certain concepts of semiconductor device physics.⁵ This concept has been used for frequency-dependent optically-induced lifetime measurements by Nakhmanson¹³, Kamieniecki,¹⁴ and by Munukata et al.¹⁵ We use the equivalent circuit of Fig. 5 to represent the semiconductor under ac light excitation. The monochromatic, ac-modulated light generates the photocurrent I_{ph} . The capacitance C_{scr} represents the surface charge-induced space-charge region. The conductances G represent the various loss mechanisms in the semiconductor. The losses occur when carriers recombine or are generated as illustrated in Fig. 4. Excess carriers at the surface recombine through surface states with a surface recombination velocity s_r , shown by conductance G_s . Thermal generation in the space-charge region as well as in the quasi-neutral bulk region is shown by $G_{g,scr}$ and $G_{g,qnr}$ and recombination in the scr and qnr regions as $G_{r,scr}$ and $G_{r,qnr}$.

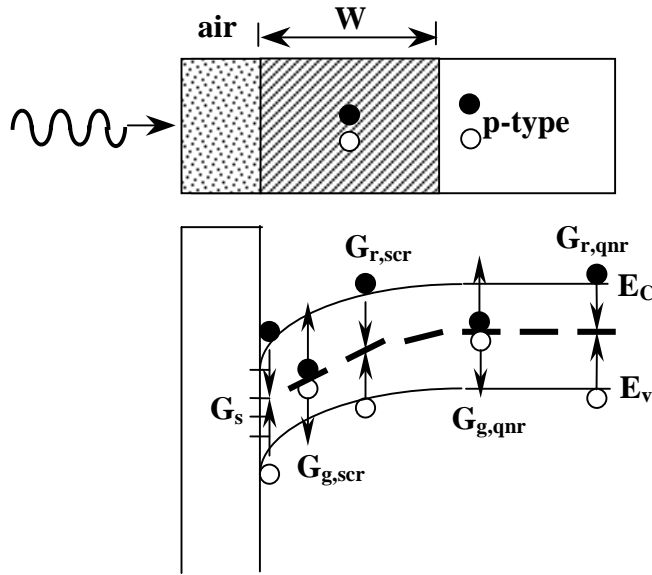


Fig. 4 The sample geometry and the conductances due to generation and recombination of excess carriers.

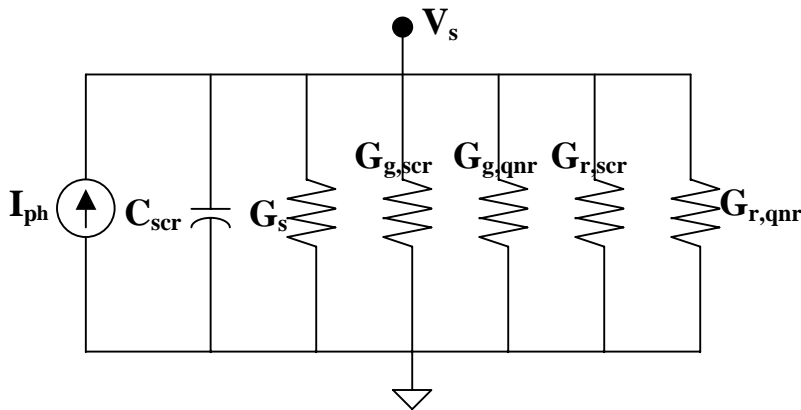


Fig. 5 The equivalent circuit for SPV measurements.

We consider a p -type substrate and concentrate on the behavior of the minority electrons. The surface recombination velocity s_r depends strongly on the surface condition. It is defined through the expression

$$D_n \frac{d(\delta n)}{dx} = s_r \delta n \quad (2)$$

where D_n is the electron diffusion coefficient and δn the small-signal excess carrier density.

We define conductances as current density divided by voltage in units of S/cm². The surface conductance G_s due to surface recombination is given by

$$G_s = \frac{J_s}{V} \approx \frac{qD_n d(\delta n)/dx}{V_{SPV}} = \frac{qs_r \delta n}{V_{SPV}} = \frac{qs_r n_{po} [\exp(qV_{SPV}/kT) - 1]}{V_{SPV}} \approx \frac{q^2 s_r n_{po}}{kT} = \frac{q^2 s_r n_i^2}{kTN_{A,epi}} \quad (3)$$

where n_{po} is the minority carrier density. The approximation in Eq. (3) obtains for low surface photovoltage, *i.e.*, $V_{SPV} < kT/q$. The “generation” conductance G_g is given by⁵

$$G_g = G_{g,scr} + G_{g,qnr} = \frac{2qK_s \epsilon_o n_i}{\tau_g N_{A,epi} W} + \frac{q\mu_n n_i^2}{N_{A,epi} L_n} \quad (4)$$

with the diffusion length given by $L_n = (D_n \tau_r)^{1/2}$, where τ_r is the recombination lifetime in the quasi-neutral region.

Carrier injection over a slightly forward-biased barrier leads to recombination in the space-charge region and to the conductance $G_{r,scr}$

$$G_{r,scr} = \frac{J_{r,scr}}{V_{SPV}} \approx \frac{\frac{qn_i W}{\tau_{scr}} (\exp(\frac{qV_{SPV}}{kT}) - 1)}{V_{SPV}} \approx \frac{q^2 n_i W}{\tau_{scr} kT} \quad (5)$$

which depends on n_i , $N_{A,epi}$, W , and the scr recombination lifetime, τ_{scr} . The qnr recombination conductance ($G_{r,qnr}$) due recombination in the quasi-neutral region is given by

$$G_{r,qnr} = \frac{J_{r,qnr}}{V_{SPV}} \approx \frac{\frac{qn_i^2 D_n}{N_A L_n} (\exp(\frac{qV_{SPV}}{kT}) - 1)}{V_{SPV}} \approx \frac{q^2 n_i^2 D_n}{N_{A,epi} L_n kT} = \frac{q\mu_n n_i^2}{N_{A,epi} L_n} \quad (6)$$

These five conductances are plotted in Fig. 6. The space-charge region recombination conductance $G_{r,scr}$ dominates for $T \leq 400K$ for the values used for that figure. The surface conductance becomes important for higher surface recombination velocity. This is similar to the scr or Sah-Noyce-Shockley recombination current dominating in Si pn junction at low voltages.

So far we have been concerned with dc behavior. Since we are ultimately interested in ac excitation, we need to consider the ac behavior of the various lifetimes. Mathematical analyses of steady-state solutions usually assume all pertinent parameters to have a “ $\exp(j\omega t)$ ” dependence, where $\omega = 2\pi f$ and f is the modulation frequency. A consequence of this modification is that the diffusion length and the lifetime become time-varying functions, defined by¹⁶

$$L_n = \frac{L_{no}}{\sqrt{1 + j\omega\tau}}; \tau = \frac{\tau_o}{1 + j\omega\tau}; s_r = s_{ro} (1 + j\omega\tau) \quad (7)$$

where L_{no} , τ_o , and s_{ro} are the dc values.

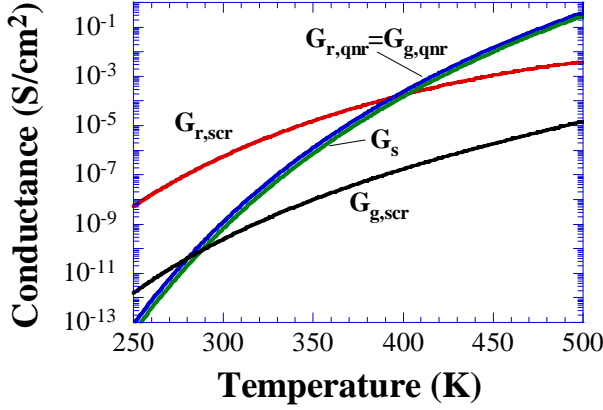


Fig. 6 Conductances versus temperature. $\tau_{scr} = 10 \mu\text{s}$, $\tau_r = 10 \mu\text{s}$, $\tau_g = 1 \text{ms}$, $s_r = 1000 \text{cm/s}$, $N_A = 10^{15} \text{cm}^{-3}$.

The recombination and generation lifetimes become $\tau_r = \tau_{ro}/(1+j\omega\tau_{ro})$ and $\tau_g = \tau_{go}/(1+j\omega\tau_{go})$. For simplicity, we have taken τ_{go} as constant with temperature, although it is approximately given by $\tau_{go} \approx \tau_{ro} \exp[(E_T - E_i)/kT]$.¹⁷ τ_{go} decreases with temperature, according to this equation, but since generally we do not know $E_T - E_i$ we have neglected this dependence here. Our results indicate that neither the capacitance nor the conductance is sensitive to the generation lifetime for the conditions we use.

To determine the frequency-dependent nature of the equivalent circuit, we consider the impedance Z of the circuit in Fig. 5. It is given by

$$Z = \frac{1}{G_{tot} + j\omega C_{scr}} \quad (8)$$

where

$$G_{tot} = G_s + G_{r,scr} + G_{r,qnr} + G_{g,scr} + G_{g,qnr}; C_{scr} = K_s \epsilon_o / W \quad (9)$$

The phase angle θ is given by

$$\theta = \tan^{-1}(X / R) \quad (10)$$

where X is the reactance and R the resistance, related to the impedance by

$$Z = \sqrt{R^2 + X^2} \quad (11)$$

The photocurrent can only flow internally in the sample since the surface is separated from the voltage probe. The electrode measures the barrier lowering or the surface photovoltage V_{SPV} shown in Fig. 3. The photocurrent in the space-charge region is¹

$$J_{ph,scr} = q\Phi(1 - R)(1 - \exp(-\alpha W)) \quad (12)$$

and the photocurrent in the quasi-neutral region of thickness t , uniformly doped with diffusion length L_n , is

$$J_{ph,qnr} = \frac{q\Phi(1-R)\alpha L_n \exp(-\alpha W)}{\alpha^2 L_n^2 - 1} \left[\alpha L_n - \frac{k_n \cosh(\phi) + \sinh(\phi) - (k_n - \alpha L_n) \exp(-\alpha d)}{\cosh(\phi) + k_n \sinh(\phi)} \right] \quad (13)$$

giving the total photocurrent as

$$J_{ph} = J_{ph,scr} + J_{ph,qnr} \quad (14)$$

where $k_n = s_r L_n / D_n$ and $\phi = t / L_n$. For epitaxial wafers with two different doping densities and very likely two different diffusion lengths, the $J_{ph,qnr}$ expression becomes more complicated. For light with high absorption coefficient, appropriate for our experimental conditions, $J_{ph,scr}$ dominates over $J_{ph,qnr}$ and $J_{ph} \approx J_{ph,scr}$. The current density depends on the photon flux density Φ , the reflectivity R , the absorption coefficient α , the layer thickness t_{epi} , the scr width W , the diffusion length L_n , and the surface recombination velocity s_r at the epi-substrate interface.

The surface photovoltage is

$$V_{SPV} = J_{ph} Z \quad (15)$$

The surface voltage and phase angle θ are plotted in Fig. 7 versus radial frequency as a function of temperature. For our measurements the excitation wavelength has an absorption coefficient of $2 \times 10^4 \text{ cm}^{-1}$, leading to an absorption depth $1/\alpha$ of $0.5 \text{ }\mu\text{m}$ with most of the light absorbed in the space-charge region.

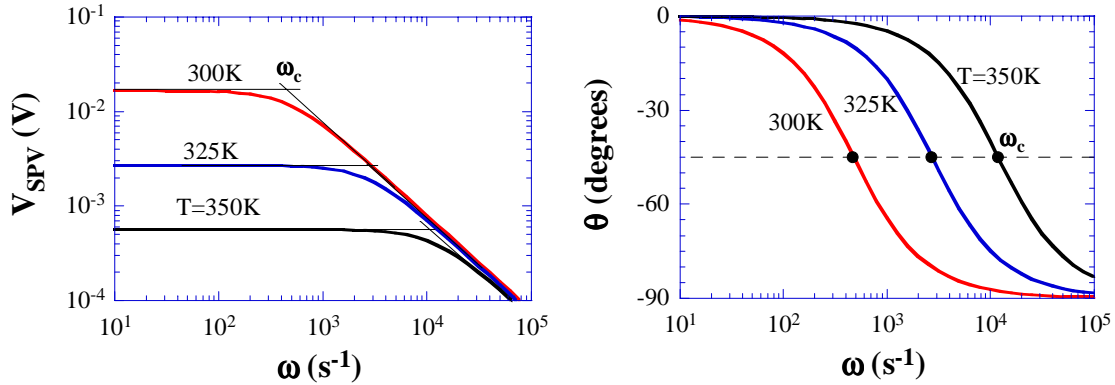


Fig. 7 V_{SPV} and θ versus ω as a function of temperature for $\Phi = 10^{12} \text{ cm}^{-2}\text{s}^{-1}$, $R = 0.3$, $\alpha = 2 \times 10^4 \text{ cm}^{-1}$, $W = 0.8 \text{ }\mu\text{m}$, $\tau_{scro} = 10^{-6} \text{ s}$, $\tau_{ro} = 10^{-5} \text{ s}$, $\tau_{go} = 10^{-3} \text{ s}$, $s_{ro} = 1000 \text{ cm/s}$, $N_{A,epi} = 10^{15} \text{ cm}^{-3}$.

An important question is: what is the effect of optical excitation? Do not the optically generated carriers interfere with lifetime measurements? To answer these questions we will consider the device impedance and how that impedance is modified by light. Impedances are most commonly measured with electrical excitation, where the device is excited with a current and the resulting voltage is measured. To understand the measurement with optical excitation, we simplify the circuit of Fig. 5 to that in Fig. 8, where G represents the five conductances from Fig. 5 while G_{ph} represents the photoconductance.

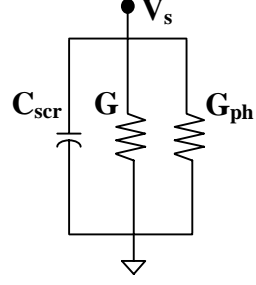


Fig. 8 Simplified equivalent circuit.

The impedance of the circuit in Fig. 8 is

$$Z = \frac{1}{G + G_{ph} + j\omega C_{scr}} \quad (16)$$

The conductances are defined as

$$G = \frac{J}{V} = \frac{q \int R dx}{V}; \quad G_{ph} = \frac{J_{ph}}{V} \quad (17)$$

where R is the recombination/generation rate. The photocurrent density should be low compared to the current density, *i.e.*,

$$J_{ph} = q\eta\Phi < q \int R dx \quad (18)$$

where η is the quantum efficiency. Equation (18) leads to

$$\Phi < \frac{\int R dx}{\eta} = \frac{qn_i W V_{SPV}}{kT\eta\tau_{r,scr}} \approx \frac{n_i W}{\eta\tau_{r,scr}} \quad (19)$$

for scr recombination being the dominant term, as shown earlier. The approximation holds for $V_{SPV} \approx kT/q$, as is typical for surface photovoltage measurements. Using $n_i = 10^{10} \text{ cm}^{-3}$, $W = 10^{-4} \text{ cm}$, $\tau_{r,scr} = 10^{-6} \text{ s}$, and $\eta = 0.5$, leads to $\Phi < 2 \times 10^{12} \text{ photons/cm}^2\text{-s}$. This restriction is relaxed at elevated temperatures. For example, at $T = 100^\circ\text{C}$, $n_i = 1.4 \times 10^{12} \text{ cm}^{-3}$ leading to $\Phi < 3 \times 10^{14} \text{ photons/cm}^2\text{-s}$.

Effect of Lifetimes

The surface photovoltage obviously depends on the various lifetimes, but which lifetime has the major effect on the surface photovoltage? To answer that question, we have calculated the effects of the various lifetimes. Varying the qnr lifetime τ_{qnr} from 10^{-6} to 10^{-3} s has almost no effect for $\tau_{scro} = 10^{-6} \text{ s}$, but does have a small effect for $\tau_{scro} = 10^{-3} \text{ s}$. The influence of the generation lifetime τ_{go} is only observed for $\tau_{scro} = 10^{-4}\text{-}10^{-3} \text{ s}$. Since τ_{go} is usually higher than τ_{scro} , it is obvious that τ_{go} also has minimal effect on V_{SPV} . Varying s_r from 10^2 to 10^7 cm/s has a significant effect on the curves. The message here is clearly that space-charge region recombination at the surface and in the space-charge

region are the dominant mechanisms. This, of course, makes it difficult to characterize the epi layer itself, unless surface recombination is minimized. For the case that surface recombination is small compared to scr recombination, $G_{r,scr}$ dominates and Eq. (9) becomes

$$G_{tot} \approx G_{r,scr} = \frac{q^2 n_i W}{\tau_{scr} kT} \quad (20)$$

with $\tau_{scr} = \tau_{scro}/(1+j\omega\tau_{scro})$.

The impedance now becomes

$$Z \approx \frac{G_{r,scr}^{-1}}{1 + j\omega C_{scr} / G_{r,scr}} = \frac{kT\tau_{scro}}{q^2 n_i W (1 + j\omega / \omega_c)} \quad (21)$$

where the corner-frequency, ω_c , is

$$\omega_c = \frac{G_{r,scr}}{C_{scr}} = \frac{q^2 n_i W^2}{kTK_s \epsilon_o \tau_{scro}} \quad (22)$$

τ_{scro} related to the corner frequency through the expression

$$\tau_{scro} = \frac{q^2 n_i W^2}{\omega_c kTK_s \epsilon_o} = \frac{5.97 \times 10^{-6} n_i W^2}{\omega_c (T/300)} \quad (23)$$

Experimental Results

ac-SPV

We have characterized epitaxial wafers with two different doping profiles. The p/p^+ sample consists of an epitaxial layer, doped to 10^{15} cm^{-3} , deposited on a highly doped substrate, doped to 10^{18} cm^{-3} . The p/p^- sample consists of an epitaxial layer, doped to 10^{15} cm^{-3} , grown on a moderately doped substrate, doped to 10^{15} cm^{-3} . The epitaxial layer thicknesses are 5 μm and 10 μm for both samples. The frequency and temperature dependence of the surface photovoltage of the 10 μm , p/p^+ sample are shown in Fig. 9. The agreement between theory and experiment is excellent. The lifetime τ_{scro} had to be changed from $0.95 \times 10^{-6} \text{ s}$ at 300K to $1.35 \times 10^{-6} \text{ s}$ at 330 K for theory and experiment to agree, consistent with lifetime increasing with increasing temperature in silicon.

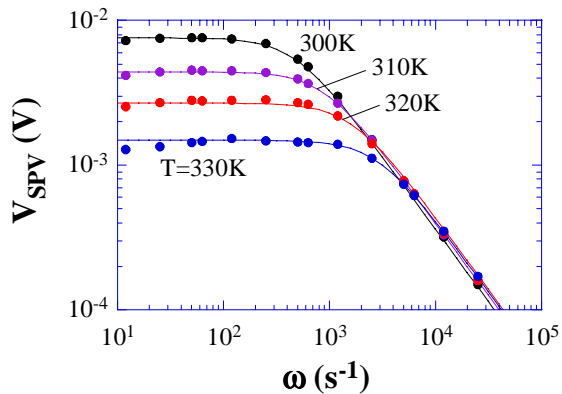


Fig. 9 Surface photovoltage versus frequency as a function of temperature.

Experiment: $t_{epi} = 10 \mu\text{m}$, $N_{A,epi} = 10^{15} \text{ cm}^{-3}$, $N_{A,sub} = 10^{18} \text{ cm}^{-3}$.

Theory: $\alpha = 2 \times 10^4 \text{ cm}^{-1}$, $W = 0.8 \mu\text{m}$, $\tau_{ro} = 10 \mu\text{s}$, $\tau_{go} = 1 \text{ ms}$, $s_{ro} = 50 \text{ cm/s}$, $N_{A,epi} = 10^{15} \text{ cm}^{-3}$.

We find the theoretical values to be relatively insensitive to τ_{ro} , the recombination lifetime in the quasi-neutral region and to τ_{go} , the generation lifetime in the space-charge region. However, they are very sensitive to τ_{scro} , the recombination lifetime in the scr and s_{ro} , the surface recombination velocity. One would expect this, for the high-absorption coefficient light generates ehps mainly generated in the scr and recombination in that region ought to dominate. Hence, the frequency response is primarily determined by τ_{scro} and s_{ro} and, in general, it is difficult to determine either one. For *low* surface recombination, the measurement does indeed characterize the epi layer through the scr recombination lifetime.

The effects of substrate doping density and epi layer thickness are shown in Fig. 10. Fig. 10(a) shows experimental data and theoretical curves for 300 K and Fig. 10(b) for 330 K. The agreement between experimental data and our theory is excellent in all cases. The space-charge recombination lifetimes range from 0.8 to 1.35 μ s. In all cases, the lifetime increases with increasing temperature. The lifetimes of the p/p^+ samples are very similar to those for the p/p^- samples for both thicknesses. The effect of heavily-doped p^+ substrates acting as getters for heavy metals like iron¹⁸ is not observed here.

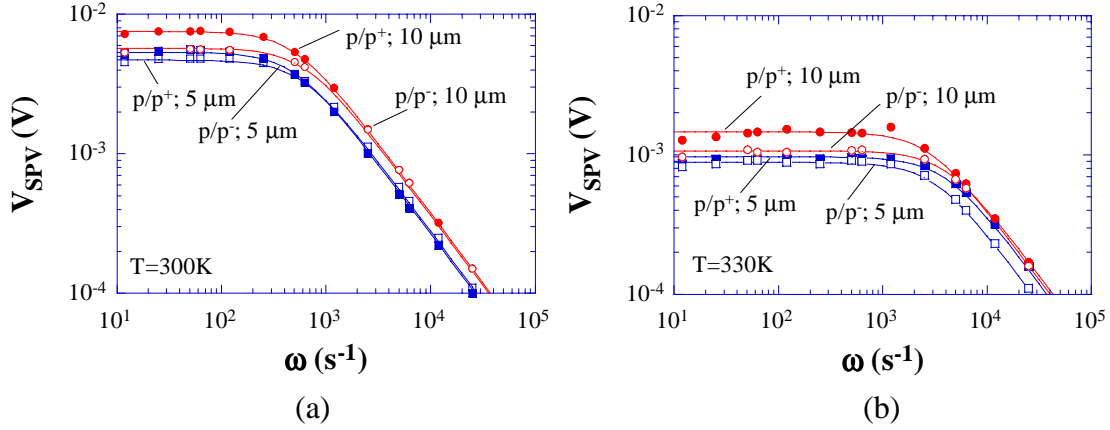


Fig. 10 Surface photovoltage versus frequency. $\tau_{go} = 1$ ms, $\tau_{ro} = 10$ μ s, $s_r = 50$ cm/s.

dc-SPV

To compare the corona charge method with conventional surface photovoltage diffusion length measurements, we measured the diffusion length of both epitaxial wafers (p/p^+ : $10^{15}/10^{18}$ cm^{-3} ; p/p^- : $10^{15}/10^{15}$ cm^{-3}). In these measurements, photons with low absorption coefficients are used leading to carrier excitation through the epitaxial layer and a significant portion of the substrate. It has been shown that in that case, it is mainly the thickness of the epitaxial layer that is measured, if the diffusion length of the substrate is significantly lower than that of the p^+ layer, as it would be for the p/p^+ samples.¹⁹ We find the following results: p/p^+ - 5 μ m layer: $L_n = 4.5$ μ m, p/p^+ - 10 μ m layer: $L_n = 7$ μ m, p/p^- - 5 μ m layer: $L_n = 330$ μ m, p/p^- - 10 μ m layer: $L_n = 304$ μ m. For the p/p^+ samples, the diffusion lengths are indeed approximately equal to the layer thicknesses, while for the p/p^- samples there is no relationship with thickness, as expected.

Conclusions

We have developed the theory to interpret ac surface photovoltage data measured in the frequency domain. The frequency-dependent behavior is a function of the scr

width, doping density, photon flux density, absorption coefficient, generation/recombination lifetime, and temperature. The corner-frequency of surface photovoltage versus frequency plots, ω_c , provides the scr recombination lifetime and surface recombination velocity with no appreciable contribution from the quasi-neutral region or the substrate. For low surface recombination velocity, the epi layer can indeed be characterized with this technique.

Acknowledgments

The research leading to this paper was partially funded by the Silicon Wafer Engineering and Defect Science Consortium (SiWEDS) (Intel, Komatsu Electronic Metals, MEMC Electronic Materials, Mitsubishi Silicon, Nippon Steel, Okmetic, Sumitomo Sitix Silicon, Texas Instruments and Wacker Siltronic Corp.).

References

-
- ¹ D.K. Schroder, *Semiconductor Material and Device Characterization*, Second Ed., Wiley-Interscience, New York, 1998.
 - ² T. Pavelka and Z. Batari, "Lifetime Measurements in SOI and Epi Structures," in *Analytical and Diagnostic Techniques for Semiconductor Materials, Devices, and Processes* (B.O. Kolbesen, C. Claeys, P. Stallhofer, F. Tardiff, J. Benton, T. Shaffner, D. Schroder, S. Kishino, and P. Rai-Choudhury, eds.), Electrochem. Soc. **ECS PV 99-16**, 48-55, 1999.
 - ³ C. Claeys, E. Simoen, A. Poyai, and A. Czerwinski, "Electrical Quality Assessment of Epitaxial Wafers Based on p-n Junction Diagnostics," *J. Electrochem. Soc.* **146**, 3429-3434, Sept. 1999.
 - ⁴ S.Y. Lee and D.K. Schroder, "Thin p/p⁺ Epitaxial Layer Characterization With the Pulsed MOS Capacitor," *Solid State Electron.* **43**, 103-111, Jan. 1999.
 - ⁵ D.K. Schroder, J.E. Park, S.E. Tan, B.D. Choi, S. Kishino, and H. Yoshida, "Frequency Domain Lifetime Characterization," *IEEE Trans. Electron Dev.*, accepted for publication.
 - ⁶ D.K. Schroder, M.S. Fung, R.L. Verkuil, S. Pandey, W.H. Howland, and M. Kleefstra, "Corona-Oxide-Semiconductor Generation Lifetime Characterization," *Solid-State Electr.* **42**, 505-512, April 1998.
 - ⁷ E. Kamieniecki, "Non-contact Measurements of the Minority Carrier Recombination Lifetime at the Silicon Surface," in *Recombination Lifetime Measurements in Silicon* (D.C. Gupta, F.R. Bacher, and W.M. Hughes, eds), ASTM **STP 1340**, 147-155, 1998.
 - ⁸ P. Renaud and A. Walker, "Measurement of Carrier Lifetime: Monitoring Epitaxy Quality," *Solid State Technol.* **43**, 143-146, June 2000.
 - ⁹ Lord Kelvin, "On a Method of Measuring Contact Electricity," *Nature*, April 1881; "Contact Electricity of Metals," *Phil. Mag.* **46**, 82-121, 1898.
 - ¹⁰ L. Kronik and Y. Shapira, "Surface Photovoltage Phenomena: Theory, Experiment, and Applications", *Surf. Sci. Rep.* **37**, 1-206, Dec. 1999.
 - ¹¹ Semiconductor Diagnostics, Inc. Manual "Contamination Monitoring System Based on SPV Diffusion Length Measurements," SDI, 1993.
 - ¹² E.O. Johnson, "Large-Signal Surface Photovoltage Studies With Germanium," *Phys. Rev.* **111**, 153-166, July 1958.
 - ¹³ R.S. Nakhmanson, "Frequency Dependence of the Photo-EMF of Strongly Inverted Ge and Si MIS Structures – I. Theory," *Solid-State Electron.* **18**, 617-626, 1975; "Frequency Dependence of the Photo-EMF of Strongly Inverted Ge and Si MIS Structures – II. Experiment," *Solid-State Electron.* **18**, 627-634, July/Aug. 1975.

-
- ¹⁴ E. Kamieniecki, "Surface Photovoltage Measured Capacitance: Application to Semiconductor/Electrolyte System," *J. Appl. Phys.* **54**, 6481-6487, Nov. 1983.
- ¹⁵ C. Munakata, S. Nishimatsu, N. Homma, and K. Yagi, "AC Surface Photovoltages in Strongly-Inverted Oxidized p-Type Silicon Wafers," *Japan. J. Appl. Phys.* **11**, 1451-1461, Nov. 1984; C. Munakata and S. Nishimatsu, "Analysis of ac Surface Photovoltages in a Depleted Oxidized p-Type Silicon Wafer," *Japan. J. Appl. Phys.* **25**, 807-812, June 1986.
- ¹⁶ J.P. McKelvey, *Solid State and Semiconductor Physics*, Harper and Row, New York, 1966.
- ¹⁷ D.K. Schroder, "The Concept of Generation and Recombination Lifetimes in Semiconductors," *IEEE Trans. Electron Dev.* **ED-29**, 1336-1338, Aug. 1982.
- ¹⁸ A.L. Smith, K. Wada, and L.C. Kimerling, "Modeling of Transition Metal Redistribution to Enable Wafer Design for Gettering," *J. Electrochem. Soc.* **147**, 1154-1160, March 2000.
- ¹⁹ J.W. Slotboom and M.J.J. Theunissen, "Impact of Silicon Substrates on Leakage Current," *IEEE Electron Dev. Lett.* **EDL-4**, 403-406, Nov. 1983; D.K. Schroder, "Effective Lifetimes in High Quality Silicon Devices," *Solid State Electron.* **27**, 247-251, March 1984; C.W. Pearce and R.J. Jaccodine, "An Analytical Model of Diffusion Current in Intrinsically Gettered Structures Based on Intentional Experiments," *IEEE Trans. Electron Dev.* **38**, 2155-2160, Sept. 1991.